PAPER

Check for updates

From oxides to oxysulfides: the mixed-anion GeS₃O unit induces huge improvement in the nonlinear optical effect and optical anisotropy for potential nonlinear optical materials†

Xinyu Tian,‡ Xiaodong Zhang,‡ Yan Xiao,‡ Xiaowen Wu, ID * Bingbing Zhang, ID Daqing Yang ID and Kui Wu ID *

Oxysulfides combining intrinsic performance advantages between sulfides (strong NLO response) and oxides (wide optical bandgap) are proposed as potential infrared (IR) NLO materials. Theoretical calculation shows that the mixed-anion GeS₃O tetrahedron has a stronger polarizability anisotropy and hyperpolarizability than that of the typical GeO₄ unit. Based on this, two $Sr_2MGe_2S_6O$ (M = Zn, Cd) oxysulfides with the GeS₃O unit show dozens of times improvement in critical birefringence and the NLO effect compared with those of isostructural $Sr_2ZnGe_2O_7$. Moreover, structure–property study further verifies that the mixed-anion GeS₃O ligand is a useful NLO-active unit and can offer great influence over the NLO origin. This research result also gives us a feasible design strategy and research system to explore new IR NLO candidates.

Nonlinear optical (NLO) crystals have shown extensive applications in extending the conventional laser wavelengths to unusual short deep-ultraviolet (DUV) or mid- and far infrared (MFIR) regions through frequency-conversion technology.[1–4] As for the IR region, inherent performance drawbacks (low laser damage threshold (LDT) and harmful two-photon absorption (TPA)) in commercial NLO crystals have seriously limited their applications.[5] As we know, the optical bandgap is proportional to the LDT but shows an inverse relationship with the NLO response; thus, it is extremely challenging to design new promising IR NLO crystals with balanced performances, such as wide bandgap (≥3.0 eV) and large second harmonic generation (SHG) effect (≥0.5 × AgGaS₂).[6] Recently, researchers have proposed several feasible design strategies to regulate the crystal structures and performances. Incorporation of mixed-anion functional groups into crystal structure was regarded as one good way to solve the above problem.[7] Based on this, several of chalcohalides have been synthesized and shown the excellent performances compared with halogen-free analogues.[8] Nowadays, oxysulfides have been also attracted increasing attentions because this system can be viewed as the modification of

sulfides and oxides, and oxysulfides exhibit the performance advantages in both of them (good NLO response and wide bandgap).[9] Besides, chalcohalides often appear the structural changes by anion-substitution of S^{2-} with halogen (X^{-}) owing to different valence states, but the atom substitution with same valence (such as O^{2-} to S^{2-}) can maintain the similar structural features, thus, oxysulfide system provides one good way to investigate the influence of mixed-anion ligand on property while compared with their isostructural oxides. With this in mind, two oxysulfides $Sr_2MGe_2S_6O$ (M = Zn, Cd) were successfully synthesized and their properties were systematically compared with $Sr_2MGe_2O_7$ in this work. Among them, crystal structure of $Sr_2ZnGe_2S_6O$ was reported in 1985 but its performances have not been studied so far.[10] Besides, optical performances of $Sr_2CdGe_2S_6O$ were reported in the Lin's master's thesis in 2019.[11] However, in view of the similar structures between $Sr_2MGe_2S_6O$ oxysulfides and $Sr_2ZnGe_2O_7$ oxides, this is good case to compare the performance change rule and study the inherent ligand-property relationship, such as from typical GeO₄ to mixed-anion GeS₃O unit. Herein, we have done the detailed performance comparison between title oxysulfides and isostructural oxides based on experimental and theoretical methods. Critical performances in $Sr_2MGe_2S_6O$ (such as optical anisotropy and SHG response) show the obvious enhancement compared with those of $Sr_2ZnGe_2O_7$, which indicates that oxysulfides have good potential to be used as IR NLO candidates.

$Sr_2MGe_2S_6O$ (M = Zn, Cd) crystallize in the tetragonal $P\bar{4}21m$ space group (Table S1†). Among them, we have chosen $Sr_2CdGe_2S_6O$ as the representative to discuss their structural

College of Chemistry and Environmental Science, Hebei University, Baoding, China. E-mail: wuxiaowen1114@163.com; wukui@hbu.edu.cn

‡ Xinyu Tian, Xiaodong Zhang and Yan Xiao contributed equally.

features (Fig. 1). In its asymmetric unit, there is composed of one Sr, one Cd, one Ge, one O and two S atoms (Table S2†). Ge atom exhibits the four-coordination mode with one O and three S atoms to form mixed-anion GeS_3O tetrahedron with $d(Ge-S) = 2.147-2.206$ Å and $d(Ge-O) = 1.834$ Å (Fig. 1d). Two GeS_3O units link together by sharing one O atom to compose the isolated Ge_2S_6O dimer. Typical CdS_4 units link with Ge_2S_6O dimers to form the two-dimensional (2D) $[CdGe_2S_{10}O]$ layers (Fig. 1e). Sr atoms connect with one O and seven S atoms to form the SrS_7O dodecahedron with $d(Sr-S) = 3.014-3.278$ Å and $d(Sr-O) = 2.829$ Å (Fig. 1c). SrS_7O units are located at the interlayers and further link with these 2D layers to form a 3D network (Fig. 1b). From another point of view, Sr atoms are located within the tunnels seen from the c-axis (Fig. 1a). $Sr_2MGe_2S_6O$ are isostructural and their whole structures are composed of 2D $[MGe_2S_{10}O]$ layers and Sr atoms are located within the interlayers. Note that MS_4 (M = Zn, Cd) are regular tetrahedral units and one MS_4 unit is connected with four (Ge_2S_6O) dimers to form the windmill shapes. We have added the structural diagrams of $Sr_2MGe_2S_6O$ from the same direction (along the c-axis) (Fig. S1†). Compared with the distortion degree of GeS_3O unit, they have the tiny differences, such as $\Delta d = 5.42 \times 10^{-3}$ in $Sr_2CdGe_2S_6O$ and $\Delta d = 5.05 \times 10^{-3}$ in $Sr_2ZnGe_2S_6O$. Besides, ZnS_4 and CdS_4 can be viewed as the regular tetrahedral units with the same $d(Zn-S) = 2.327$ Å and $d(Cd-S) = 2.494$ Å. We have surveyed the compounds with O–Ge–S tetrahedron based on the Inorganic Crystal Structure Database and the result shows that $MGeOS_2$ (M = Sr, Ba)[9g] have another special GeO_2S_2 unit and these GeO_2S_2 units further link together to compose the $(GeO_2S_2)_n$ chains, which is different with that (isolated Ge_2S_6O dimer) in $Sr_2MGe_2S_6O$. Note that GeO_2S_2 unit shows close relationship with SHG effect but the specific contribution of GeS_3O unit on the SHG origin has not been studied. In view of the disparity

between Ge–S and Ge–O bond length, GeS_3O exhibits the higher distortion degree than that of GeO_4, which is conducive to the generation of large SHG response.

Microcrystals of $Sr_2MGe_2S_6O$ were successfully synthesized in vacuum-sealed silica tubes and their experimental powder XRD patterns are in consistence with corresponding calculated ones (Fig. 2a and b). Their polycrystalline samples show the good chemical stability and can be stably stored in air more than half a year. We have also investigated their thermal behaviour and measured the differential thermal curves in the customized tiny silica tubes. $Sr_2MGe_2S_6O$ have the explicit endothermic and exothermic peaks in the heating and cooling process, for example, $Sr_2ZnGe_2S_6O$ has the single melting temperature (1030 °C) and crystallization point (832 °C), whereas the melting and crystallization points of $Sr_2CdGe_2S_6O$ are 941 and 776 °C, respectively (Fig. 2c and d). We have also studied the XRD patterns before and after recrystallization process and they still have the similar XRD patterns, which verifies that $Sr_2MGe_2S_6O$ are congruent-melting compounds (Fig. 2a and b). Thus, $Sr_2MGe_2S_6O$ oxysulfides could be grown as large-size single-crystals by the conventional Bridgman–Stock-barger (BS) method. Their diffuse-reflection spectra were measured and their experimental bandgaps are 3.30 eV for $Sr_2ZnGe_2S_6O$ (colorless) and 3.13 eV for $Sr_2CdGe_2S_6O$ (pale-yellow) (Fig. 2e), respectively, which are smaller than that of $Sr_2ZnGe_2O_7$ (4.31 eV) (Fig. S2 and S3†). First principles calculation was used to analyze the inherent structure–property relationship.[12] Seen from their electronic structures, $Sr_2MGe_2S_6O$ are indirect bandgap compounds and their theoretical bandgaps are calculated to be 2.77 and 2.67 eV, respectively (Fig. 3a and b), such theoretical values are often estimated due to the GGA calculation problem. Besides, they have the similar density of states (DOS) and $Sr_2ZnGe_2S_6O$ was chosen as representative to be discussed (Fig. 3c and d). Near the top of valence band (VB: −5 to 0 eV), this region is mainly composed of S-p orbital with minor contribution from Ge-p and Zn-p orbitals. On the bottom of conduction band (CB), Zn-s, Ge-s, Ge-p and S-p orbitals produce the major contribution on this region, thus, optical absorption of $Sr_2ZnGe_2S_6O$ can be attributed as the synergistic effect between ZnS_4 and GeS_3O units. Compared with the DOS diagram of $Sr_2ZnGe_2O_7$ (Fig. S5†), S-p orbital makes the great influence on the Fermi-level and further induces the obvious red shift of short absorption edge in $Sr_2ZnGe_2S_6O$.

In view of the isostructural NCS structures between $Sr_2MGe_2S_6O$ and $Sr_2ZnGe_2O_7$, their powder SHG responses have been tested with a 2.09 μm Q-switch pulse laser and commercial $AgGaS_2$ was chosen as the reference (Fig. 2f). SHG signal intensities of $Sr_2MGe_2S_6O$ show the continuously increasing trend with the enhanced particle sizes range from 38 to 250 μm, which shows that they satisfy the phase-matching (PM) condition. And at the maximum particle size (200–250 μm), they exhibit the good SHG responses about 0.6 for $Sr_2ZnGe_2S_6O$ and 0.7 times that of $AgGaS_2$ for $Sr_2CdGe_2S_6O$, respectively, which are comparable to those of other reported NLO oxysulfides, such as $Sr_5Ga_8O_3S_{14}$ (0.8 × $AgGaS_2$),[9d] $SrGeOS_2$ (0.4 × $AgGaS_2$)[9g] and $BaGeOS_2$ (0.5 × $AgGaS_2$)[9g] signal under the 2.09 μm about 1/20
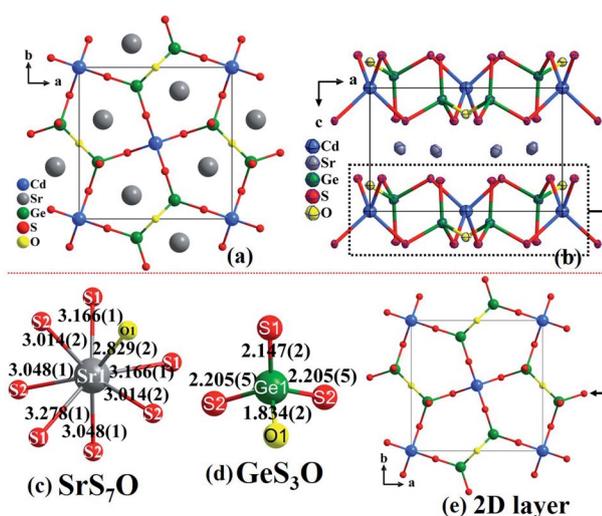

Fig. 1 (a) Crystal structure of $Sr_2CdGe_2S_6O$ seen from c-axis (Sr−S/Sr−O bonds were omitted for clearly); (b) crystal structure of $Sr_2CdGe_2S_6O$ seen from b-axis (Sr−S/Sr−O bonds were omitted for clearly); coordination modes of SrS_7O (c) and GeS_3O (d) units with bond-length (Å); (e) 2D layer composed of CdS_4 and GeS_3O units.
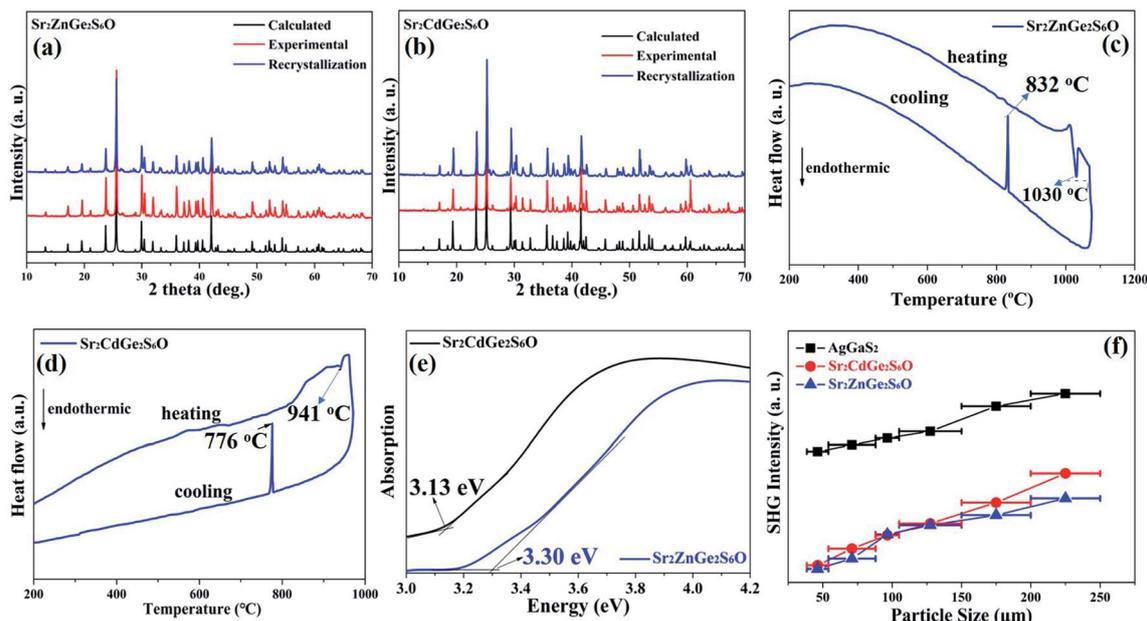
Fig. 2 Powder XRD patterns of $Sr_2ZnGe_2S_6O$ (a) and $Sr_2CdGe_2S_6O$ (b); DSC curves of $Sr_2ZnGe_2S_6O$ (c) and $Sr_2CdGe_2S_6O$ (d); (e) optical bandgaps of $Sr_2MGe_2S_6O$; (f) SHG response *versus* particle size in $Sr_2MGe_2S_6O$ with $AgGaS_2$ as reference.

times than of $AgGaS_2$ at the maximum particle size and they cannot achieve the PM behavior (Fig. S4†). Theoretical NLO coefficients are calculated to be −3.71 for $Sr_2ZnGe_2S_6O$ and −3.53 pm V^{-1} for $Sr_2CdGe_2S_6O$, respectively, which are much larger than that (−0.144 pm V^{-1}) of $Sr_2ZnGe_2O_7$. Therefore, SHG responses of $Sr_2MGe_2S_6O$ undergo the great promotion about 25 times that of $Sr_2ZnGe_2O_7$, which agree well with the As for the previously Lin' reported $Sr_2CdGe_2S_6O$,[11] its SHG effect about 0.3 × $AgGaS_2$ was measured at one particle size at 125–150 μm. Unfortunately, $Sr_2ZnGe_2O_7$ only shows the very weak SHG data. In order to verify the specific PM condition, we have also calculated their optical anisotropy (Δn) between $Sr_2MGe_2S_6O$

and $Sr_2ZnGe_2O_7$ (Fig. S6†). The result shows that $Sr_2MGe_2S_6O$ exhibit the significant increase (0.126–0.141 @ 2 μm) about up to dozens of times that of $Sr_2ZnGe_2O_7$ (0.011 @ 2 μm), thus, mixed-anion units have a good chance to enhance the birefringence for critical phase-matching demand, which is also corresponding to the change rules of polarizability anisotropy from GeO_4 to GeS_3O ligand (Fig. 5a). SHG-density calculation (Fig. 4) was also used to analyse the origin of NLO effect in oxysulfides and their SHG responses can be attributed as the collaborative contribution from MS_4 and GeS_3O units, which
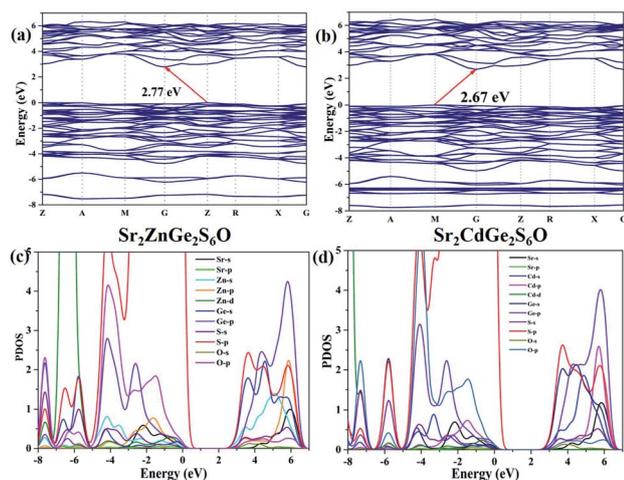

Fig. 3 (a) Band structure of $Sr_2ZnGe_2S_6O$; (b) band structure of Sr_2-$CdGe_2S_6O$; (c) PDOS diagram of $Sr_2ZnGe_2S_6O$; (d) PDOS diagram of $Sr_2CdGe_2S_6O$.
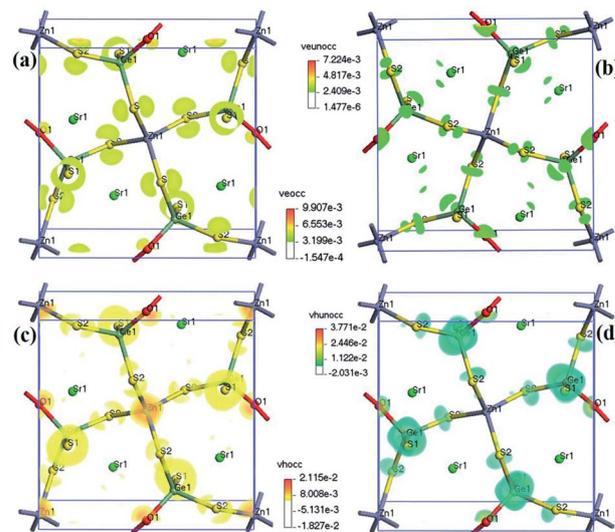

Fig. 4 SHG-density maps of $Sr_2ZnGe_2S_6O$. (a) Occupied and (b) unoccupied states in the virtual-electron (VE) process; (c) occupied and (d) unoccupied states in the virtual-hole (VH) process.
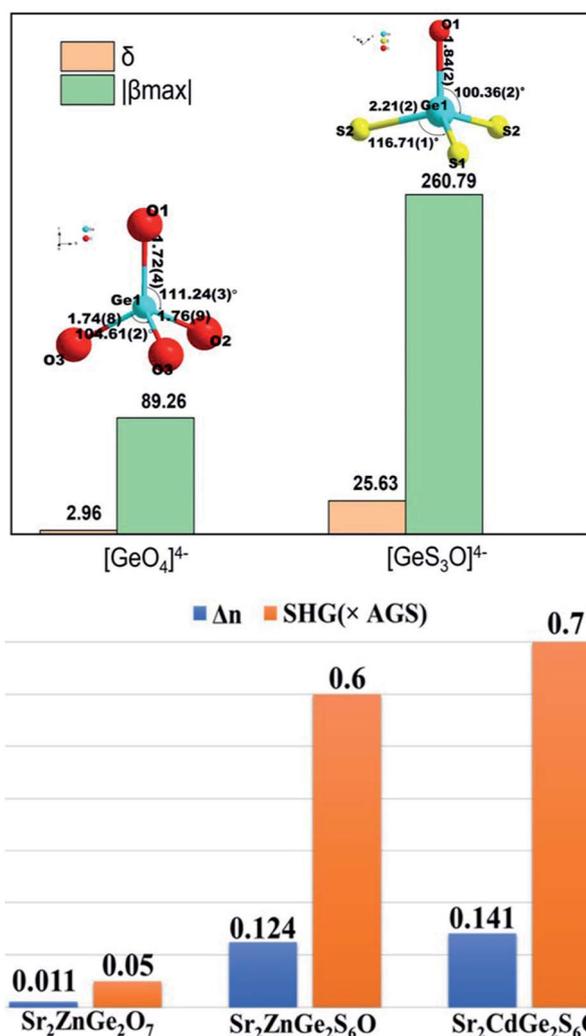
Fig. 5 Calculated hyperpolarizability (β_{max}) and polarizability anisotropy (δ) of GeO_4 and GeS_3O units (upper); property comparison between birefringence and SHG response among $Sr_2ZnGe_2O_7$ and $Sr_2MGe_2S_6O$ (lower).

indicates that GeS_3O unit is one useful NLO-active unit and offer the positive effect on the SHG origin. Moreover, gaussian calculation shows that GeS_3O exhibits the stronger hyperpolarizability (β_{max}) and polarizability anisotropy (δ) than those of GeO_4, which are consistence with the variation of experimental results from $Sr_2ZnGe_2O_7$ to $Sr_2MGe_2S_6O$ (Fig. 5). Moreover, increase optical bandgaps and decreased SHG responses were appeared from $Sr_2ZnGe_2S_6O$ to $Sr_2CdGe_2S_6O$ with the Cd was replaced with Zn atoms. This study also verifies the oxysulfides as the optimal research system for the exploring the new IR NLO materials.

Conclusions

In summary, through the partial substitution of O with S atoms in the structure of $Sr_2ZnGe_2O_7$, $Sr_2MGe_2S_6O$ IR NLO oxysulfides with specific GeS_3O unit were successfully synthesized. Research result shows that $Sr_2MGe_2S_6O$ achieve the good

balanced performances between wide bandgap (3.13–3.30 eV) and good SHG response (0.6–0.7 × $AgGaS_2$), showing the potential application as IR NLO materials. Besides, $Sr_2MGe_2S_6O$ satisfy the PM condition and their birefringence ($\Delta n = 0.126$) are much larger than that ($\Delta n = 0.011$) of $Sr_2ZnGe_2O_7$ due to the great contribution of mixed-anion units. Theoretical analysis indicates that mixed-anion GeS_3O unit offers the positive influence on the SHG origin. Furthermore, oxysulfides coexisting the property advantages between oxides and sulfides could be regarded as a good system choice for the future exploration of new IR NLO crystals.

Conflicts of interest

There are no conflicts to declare.

Acknowledgements

Notes and references

1 (a) M. Mutailipu, K. R Poeppelmeier and S. L. Pan, *Chem. Rev.*, 2021, **121**, 1130; (b) I. Chung and M. G. Kanatzidis, *Chem. Mater.*, 2014, **26**, 849; (c) T. T. Tran, H. W. Yu, J. M. Rondinelli, K. R. Poeppelmeier and P. S. Halasyamani, *Chem. Mater.*, 2016, **28**, 5238; (d) Z. G. Xia and K. R. Poeppelmeier, *Acc. Chem. Res.*, 2017, **50**, 1222; (e) G. H. Zou and K. M. Ok, *Chem. Sci.*, 2020, **11**, 5404; (f) X. F. Wang, Y. Wang, B. B. Zhang, F. F. Zhang, Z. H. Yang and S. L. Pan, *Angew. Chem., Int. Ed.*, 2017, **56**, 14119; (g) Y. Pan, S. P. Guo, B. W. Liu, H. G. Xue and G. C. Guo, *Coord. Chem. Rev.*, 2018, **374**, 464; (h) S. G. Zhao, P. F. Gong, S. Y. Luo, S. J. Liu, L. N. Li, M. A. Asghar, T. Khan, M. C. Hong, Z. S. Lin and J. H. Luo, *J. Am. Chem. Soc.*, 2015, **137**, 2207; (i) K. M. Ok, *Acc. Chem. Res.*, 2016, **49**, 2774.

2 (a) M. Luo, F. Liang, Y. X. Song, D. Zhao, N. Ye and Z. S. Lin, *J. Am. Chem. Soc.*, 2018, **140**, 6814; (b) S. S. Li, X. M. Liu, H. P. Wu, Z. F. Song, H. W. Yu, Z. S. Lin, Z. G. Hu, J. Y. Wang and Y. C. Wu, *Chem. Sci.*, 2021, **12**, 13897; (c) S. F. Li, X. M. Jiang, Y. H. Fan, B. W. Liu, H. Y. Zeng and G. C. Guo, *Chem. Sci.*, 2018, **9**, 5700; (d) P. Becker, *Adv. Mater.*, 1998, **10**, 979; (e) L. Xiong, J. Chen, J. Lu, C. Y. Pan and L. M. Wu, *Chem. Mater.*, 2018, **30**, 7823; (f) D. H. Lin, M. Luo, C. S. Lin, F. Xu and N. Ye, *J. Am. Chem. Soc.*, 2019, **141**, 3390; (g) Y. Q. Li, Z. Y. Zhou, S. G. Zhao, F. Liang, Q. R. Ding, J. L. Sun, Z. S. Lin, M. C. Hong and J. H. Luo, *Angew. Chem., Int. Ed.*, 2021, **60**, 11457; (h) C. Yang, X. Liu, C. Teng, X. Cheng, F. Liang and Q. Wu, *Mater. Today Phys.*,

2021, **19**, 100432; (*i*) L. Kang, F. Liang, X. X. Jiang, Z. S. Lin and C. T. Chen, *Acc. Chem. Res.*, 2020, **53**, 209.

3 (*a*) J. Y. Yao, D. J. Mei, L. Bai, Z. S. Lin, W. L. Yin, P. Z. Fu and Y. C. Wu, *Inorg. Chem.*, 2010, **49**, 9212; (*b*) J. Lu, J. N. Yue, L. Xiong, W. K. Zhang, L. Chen and L. M. Wu, *J. Am. Chem. Soc.*, 2019, **141**, 8093; (*c*) T. K. Bera, J. I. Jang, J. B. Ketterson and M. G. Kanatzidis, *J. Am. Chem. Soc.*, 2009, **131**, 75; (*d*) C. X. Li, X. H. Meng, Z. Li and J. Y. Yao, *Coord. Chem. Rev.*, 2022, **453**, 214328; (*e*) W. Xing, C. Tang, N. Wang, C. Li, Z. Li, J. Wu, Z. Lin, J. Yao, W. Yin and B. Kang, *Inorg. Chem.*, 2020, **59**, 18452; (*f*) J. A. Brant, D. J. Clark, Y. S. Kim, J. I. Jang, J. H. Zhang and J. A. Aitken, *Chem. Mater.*, 2014, **26**, 3045; (*g*) M. Y. Ran, Z. J. Ma, H. Chen, B. X. Li, X. T. Wu, H. Lin and Q. L. Zhu, *Chem. Mater.*, 2020, **32**, 5890.

4 (*a*) Z. J. Ma, J. Y. Hu, R. J. Sa, Q. H. Li, Y. F. Zhang and K. C. Wu, *J. Mater. Chem. C*, 2017, **5**, 1963; (*b*) Y. J. Jia, Y. G. Chen, Y. Guo, X. F. Guan, C. B. Li, B. X. Li, M. M. Liu and X. M. Zhang, *Angew. Chem., Int. Ed.*, 2019, **58**, 17194; (*c*) M. Y. Li, B. X. Li, H. Lin, Z. J. Ma, L. M. Wu, X. T. Wu and Q. L. Zhu, *Chem. Mater.*, 2019, **31**, 6268; (*d*) J. H. Zhang, D. J. Clark, J. A. Brant, K. A. Rosmus, P. Grima, J. W. Lekse, J. I. Jang and J. A. Aitken, *Chem. Mater.*, 2020, **32**, 8947; (*e*) H. Lin, W. B. Wei, H. Chen, X. T. Wu and Q. L. Zhu, *Coord. Chem. Rev.*, 2020, **406**, 213150; (*f*) H. Chen, W. B. Wei, H. Lin and X. T. Wu, *Coord. Chem. Rev.*, 2021, **448**, 214154.

5 (*a*) A. O. Okorogu, S. B. Mirov, W. Lee, D. I. Crouthamel, N. Jenkins, A. Y. Dergachev, K. L. Vodopyanov and V. V. Badikov, *Opt. Commun.*, 1998, **155**, 307; (*b*) G. D. Boyd, F. G. Storz, J. H. McFee and H. M. Kasper, *IEEE J. Quantum Electron.*, 1972, **8**, 900; (*c*) G. D. Boyd, E. Buehler and F. G. Storz, *Appl. Phys. Lett.*, 1971, **18**, 301.

6 (*a*) A. G. Jackson, M. C. Ohmer and S. R. LeClair, *Infrared Phys. Technol.*, 1997, **38**, 233; (*b*) L. Kang, M. L. Zhou, J. Y. Yao, Z. S. Lin, Y. C. Wu and C. T. Chen, *J. Am. Chem. Soc.*, 2015, **137**, 13049; (*c*) F. Liang, L. Kang, Z. S. Lin and Y. C. Wu, *Cryst. Growth Des.*, 2017, **17**, 2254.

7 Y. Y. Li, W. J. Wang, H. Wang, H. Lin and L. M. Wu, *Cryst. Growth Des.*, 2019, **19**, 4172.

8 (*a*) P. Yu, L. J. Zhou and L. Chen, *J. Am. Chem. Soc.*, 2012, **134**, 2227; (*b*) B. W. Liu, H. Y. Zeng, X. M. Jiang, G. E. Wang, S. F. Li, L. Xu and G. C. Guo, *Chem. Sci.*, 2016, **7**, 6273; (*c*) B. W. Liu, X. M. Jiang, H. Y. Zeng and G. C. Guo, *J. Am. Chem. Soc.*, 2020, **142**, 10641; (*d*) R. L. Gitzendanner and F. J. DiSalvo, *Inorg. Chem.*, 1996, **35**, 2623; (*e*) S. P. Guo, G. C. Guo, M. S. Wang, J. P. Zou, H. Y. Zeng, L. Z. Cai and J. S. Huang, *Chem. Commun.*, 2009, **29**, 4366; (*f*) Z. D. Sun, Y. Chi, H. G. Xue and S. P. Guo, *Inorg. Chem. Front.*, 2017, **4**, 1841; (*g*) K. Feng, L. Kang, Z. S. Lin, J. Y. Yao and Y. C. Wu, *J. Mater. Chem. C*, 2014, **2**, 4590; (*h*) P. F. Liu, Y. Y. Li, Y. J. Zheng, J. S. Yu, R. H. Duan, H. Chen, H. Lin, L. Chen and L. M. Wu, *Dalton Trans.*, 2017, **46**, 2715; (*i*) J. Beck, S. Hedderich and K. Kollisch, *Inorg. Chem.*, 2000, **39**, 5847.

9 (*a*) Y. F. Shi, W. B. Wei, X. T. Wu, H. Lin and Q. L. Zhu, *Dalton Trans.*, 2021, **50**, 4112; (*b*) T. Sambrook, C. F. Smura, S. J. Clarke, K. M. Ok and P. S. Halasyaman, *Inorg. Chem.*, 2007, **46**, 2571; (*c*) Y. Tsujimoto, C. A. Juillerat, W. G. Hang, K. Fujii, M. Yashima, S. Halasyamani and H. Z. Loye, *Chem. Mater.*, 2018, **30**, 6486; (*d*) R. Q. Wang, Y. W. Guo, X. Zhang, Y. Xiao, J. Y. Yao and F. Q. Huang, *Inorg. Chem.*, 2020, **59**, 9944; (*e*) R. Q. Wang, F. Liang, F. K. Wang, Y. W. Guo, X. Zhang, Y. Xiao, K. J. Bu, Z. S. Lin, J. Y. Yao, T. Y. Zhai and F. Q. Huang, *Angew. Chem., Int. Ed.*, 2019, **24**, 8078; (*f*) Y. Wang, M. J. Luo, P. Zhao, X. L. Che, Y. Z. Cao and F. Q. Huang, *CrystEngComm*, 2020, **22**, 3526; (*g*) X. Zhang, Y. Xiao, R. Q. Wang, P. X. Fu, C. Zheng and F. Q. Huang, *Dalton Trans.*, 2019, **48**, 14662.

10 T. Endo, Y. Doi, M. Wakeshima, K. Suzuki, Y. Matsuo, K. Tezuka, T. Ohtsuki, Y. J. Shan and Y. Hinatsu, *Inorg. Chem.*, 2017, **56**, 2459.

11 Y. J. Lin, Exploration of new Mid-infrared nonlinear optical materials containing transition metals, Master thesis, Fujian Normal University, China, 2019.

12 (*a*) J. P. Perdew, K. Burke and M. Ernzerhof, *Phys. Rev. Lett.*, 1996, **77**, 3865; (*b*) C. Aversa and J. E. Sipe, *Phys. Rev. B: Condens. Matter Mater. Phys.*, 1995, **52**, 14636; (*c*) M.-H. Lee, C.-H. Yang and J.-H. Jan, *Phys. Rev. B: Condens. Matter Mater. Phys.*, 2004, **70**, 235110.